Astronomy
&
Astrophysics

Reversal-free Ca II H profiles: a challenge for solar chromosphere modeling in quiet inter-network

R. Rezaei[1], J. H. M. J. Bruls[1], W. Schmidt[1], C. Beck[2], W. Kalkofen[3], and R. Schlichenmaier[1]

[1] Kiepenheuer-Institut für Sonnenphysik, Schöneckstr. 6, 79104 Freiburg, Germany
    e-mail: [rrezaei;bruls;wolfgang;schliche]@kis.uni-freiburg.de
[2] Instituto de Astrofísica de Canarias (IAC), Via Láctea, E 38 205, La Laguna, Spain
    e-mail: cbeck@iac.es
[3] Harvard-Smithsonian Center for Astrophysics, 60 Garden Street, Cambridge, MA 02138, USA
    e-mail: wolf@cfa.harvard.edu

ABSTRACT

Aims. We study chromospheric emission to understand the temperature stratification in the solar chromosphere.
Methods. We observed the intensity profile of the Ca II H line in a quiet Sun region close to the disk center at the German Vacuum Tower Telescope. We analyze over 10^5 line profiles from inter-network regions. For comparison with the observed profiles, we synthesize spectra for a variety of model atmospheres with a non local thermodynamic equilibrium (NLTE) radiative transfer code.
Results. A fraction of about 25% of the observed Ca II H line profiles do not show a measurable emission peak in H_{2v} and H_{2r} wavelength bands (reversal-free). All of the chosen model atmospheres with a temperature rise fail to reproduce such profiles. On the other hand, the synthetic calcium profile of a model atmosphere that has a monotonic decline of the temperature with height shows a reversal-free profile that has much lower intensities than any observed line profile.
Conclusions. The observed reversal-free profiles indicate the existence of cool patches in the interior of chromospheric network cells, at least for short time intervals. Our finding is not only in conflict with a full-time hot chromosphere, but also with a very cool chromosphere as found in some dynamic simulations.

Key words. Sun: chromosphere – Sun: atmosphere

1. Introduction

Solar model atmospheres are built to reproduce the observed intensity spectrum of the Sun in continuum windows and selected lines (e.g., the series of models initiated by Vernazza et al. 1981). These models rely on temporally and spatially averaged spectra. Hence, they provide information about the average properties of the physical parameters in the solar atmosphere (Linsky & Avrett 1970). At high spatial, spectral, and temporal resolution, differences from the average profiles arise, leading to different interpretations of the atmospheric stratification. In this context, there is no general agreement on the temperature stratification in the solar chromosphere. This is closely related to the fundamental problem of the heating mechanisms in the chromosphere. Carlsson & Stein (1994, 1997) proposed that apart from short-lived heating episodes in the chromosphere its time-averaged temperature stratification is monotonically decreasing with geometrical height. As noted by Carlsson et al. (1997), there are disagreements between this model and SUMER data. Moreover, the cool model was criticized by Kalkofen et al. (1999) who argued that the chromosphere is always hot and can never reach such a low activity state as proposed by Carlsson & Stein. On the other hand, Ayres (2002) challenged the arguments of Kalkofen et al. based on observations of CO lines at the solar limb. The results of the CO observations were supported by three-dimensional MHD simulations that suggested very cool structures in the upper atmosphere and implied a thermally bifurcated medium in non-magnetic regions (Wedemeyer-Böhm et al. 2004, 2005).

Recently, Avrett (2007) suggested that it is possible to reproduce a wide range of continuum and line intensities with a temperature stratification within 400 K of the semi-empirical models (Fontenla et al. 2006, and references therein). He concluded that "...these results appear to conflict with dynamical models that predict time variation of 1000 K or more in the chromosphere...".

In this paper, we comment on both full-time hot and dynamic models, based on the lowest intensity profiles we observed. We present observations and data reduction in Sect. 2. Then, we try to reproduce the observed reversal-free calcium profiles (i.e., profiles without emission peaks) by synthesizing line profiles from a variety of model atmospheres using a non local thermodynamic equilibrium (NLTE) radiative transfer code (Sects. 3 and 4). The discussion and conclusion appear in Sects. 5 and 6, respectively.

2. Observations

A quiet Sun area close to disk center ($\cos\theta = 0.99$) was observed at the German Vacuum Tower Telescope (VTT) on Tenerife, July 07, 2006. The good and stable seeing condition during the observation and the Kiepenheuer Adaptive Optics System (von der Lühe et al. 2003) provided high spatial resolution in the calcium profiles, leading to a collection of different structures observed in the quiet Sun. We used an integration time of 4.8 s and achieved a spatial resolution of 1 arcsec. Details of the observation appeared in Rezaei et al. (2007b).

The Ca II H intensity profile and Stokes vector profiles of the visible neutral iron lines at 630.15 nm, and 630.25 nm were

observed with the blue and red channels of the POlarimetric LIttrow Spectrograph (POLIS; Schmidt et al. 2003; Beck et al. 2005). POLIS was designed to provide co-temporal and co-spatial measurements of the magnetic field in the photosphere and the Ca II H intensity profile. We normalized the average calcium profile in the line wing at 396.490 nm to the Fourier Transform Spectrograph profile (Stenflo et al. 1984) and applied the calibration factor to all profiles. Details of the calibration procedure for the calcium profiles are explained in Rezaei et al. (2007a). The overall properties of the observed time-series are shown in Fig. 1 concatenated to a single map. The H-index, which is the integral of the normalized calcium profile within 0.1 nm around the core, is shown in the top panel (see Cram & Damé 1983; Lites et al. 1993, for definitions of the H-index, V and R band intensities). The middle panel shows the profile type. It is coded as follows: [0] reversal-free, [1] normal (with two emission peaks), [2] asymmetric (with only one emission peak), and [3] other types. The bottom panel of Fig. 1 shows V_{tot}, which is a measure of the signed magnetic flux (Lites et al. 1999). It is immediately seen that reversal-free profiles are absent in the vicinity of network elements ($y \sim 20$ arcsec in Fig. 1).

The top row of Fig. 2 shows three profiles belonging to different activity levels in the quiet Sun. The left profile has two red emission peaks, the middle profile shows virtually no violet emission peak and the right profile shows a strong violet and a weak red emission peak ($V/R > 2.1$). The gray profile is the average of a few thousand profiles (cell interior and boundary) with an H-index of 10.1 pm. An alternative way to measure the asymmetry of the two emission peaks is dividing the peak values rather than band integrated intensities (Rezaei et al. 2007a). In very asymmetric cases, i.e., where there is only a large violet peak, we can easily achieve a large V/R ratio with band definitions whereas the peak ratio is undefined. Double reversal calcium profiles in old observations with lower spatial resolution do not show extreme values for the ratio of the peaks. It requires both high spatial and temporal resolution and large signal to noise ratio. The maximum and minimum V/R (peak) ratio in our data set are 2.2 and 0.5 (top right and middle panels, Fig. 2). The importance of using peak values instead of bands is that the formation height of different wavelengths in the band can differ by more than one Mm (see Fig. 5 and the left panel of Fig. 6). The bottom panels of Fig. 2 show calcium profiles observed in absolutely quiet Sun regions. There is no emission peak or bulge in the core of these profiles. In the bottom row of Fig. 2, the left profile has the same wing intensity as the average profile (gray), while the middle and right profiles show lower and higher wing intensities than the average profile, respectively. Note that the reversal-free profiles usually have a V/R ratio very close to one, i.e., they are symmetric (check values in the bottom panels of Fig. 2). These reversal-free profiles were called absorption profiles by Grossman-Doerth et al. (1974). They rightly concluded that the source function of the calcium line then shows negligible enhancement in the atmospheric layers where the line forms. An emission bulge exists in the minimum profile of Cram & Damé (1983) (their Fig. 3) while this is not the case in the bottom panel, Fig. 2. This difference means that our reversal-free profiles present a new minimum state for the observed Ca II H profiles. Our observations have better spatial and temporal resolutions than Cram & Damé (1983), so we expect to find more extreme cases than these authors.

Statistics: There are many references on statistical properties of the Ca II H line profiles (e.g., Cram & Damé 1983), but our statistics on reversal-free profiles are the first. We exclude the range $y = 15-25$ arcsec in our maps because that clearly contains magnetic network. Then we perform a statistical analysis to check how often the reversal-free profiles occur. The inter-network sample has some 129 000 profiles. We check the existence of the emission peaks by analyzing the profile shape. Among the profiles that have no emission peaks, some show a strong H-index as in the top panel of Fig. 3; but others, like the bottom panels of Fig. 2, show a rather normal wing intensity and a dark core. We find that 25% of all profiles do not show any emission peak: 16% have an H-index larger than 9 pm, 8% between 8 and 9 pm, and 1% below 8 pm. Examples of calcium profiles with low H-index and no emission peak are shown in the lower panels of Fig. 2. A majority of these 25% show a tiny bulge at the position of the emission peaks.

It is worth noting that the H-index alone is not a reliable parameter for identifying the reversal-free profiles, as is demonstrated in Fig. 3. The upper profile shows no emission peaks, but the wing intensities suggest a hotter upper photosphere and a lower photospheric temperature gradient; the lower profile has two clear emission peaks, but the wing intensities demand a cooler upper photosphere. Consequently, the H-index of the bottom profile is less than half of the upper profile. This is in accordance with the fact that all three panels of Fig. 2 (bottom row) show reversal-free profiles with an H-index larger than 8 pm.

Besides the 25% fraction of reversal-free profiles in our sample, 46% of all profiles show a double reversal, with strong tendency to have a brighter violet peak. The remaining 29% of all inter-network profiles show just one emission peak, again with a majority of strong violet emission peaks, similar to previous studies (e.g., Cram & Damé 1983).

3. Synthetic calcium profiles

To reproduce the reversal-free profiles we compute synthetic Ca II H profiles by means of the NLTE radiative transfer code RH, developed by Uitenbroek (2001). The atomic model is the standard 5-level plus continuum model that is included with the RH code; apart from minor atomic data updates, this model is essentially equal to the one used by Uitenbroek (1989), which in turn dates back to Shine & Linsky (1974) and references therein. As shown by Uitenbroek (1989), partial frequency redistribution of the photons in both Ca II H&K needs to be taken into account, whereas assuming complete redistribution in the lines of the infrared triplet has no noticeable influence on the profiles of H&K. Partial redistribution makes the line source functions wavelength dependent and significantly reduces the strength of the H_2 and K_2 emission w.r.t. the common complete redistribution case. Note that since we only deal with static atmosphere models, it suffices to use angle-averaged partial frequency redistribution. Furthermore, Solanki et al. (1991) found that the width of the K_2 (and implicitly H_2) peaks correlates with the microturbulent velocities in the chromosphere. Zero microturbulence produces stronger and narrower peaks whereas the microturbulence values given with semi-empirical 1D solar models typically result in shallower, wider peaks. Microturbulence is a parameter that is used in particular in 1D radiative transfer modeling to account for the influence of spatially unresolved velocities on the line profiles. For 2D and 3D dynamic models it is generally not needed.

Since full 2D or 3D (dynamic) radiative transfer modeling is beyond current computational resources, we use static 1D plane-parallel models to synthesize Ca II H line profiles, even though the structures that we observe are so small that we expect
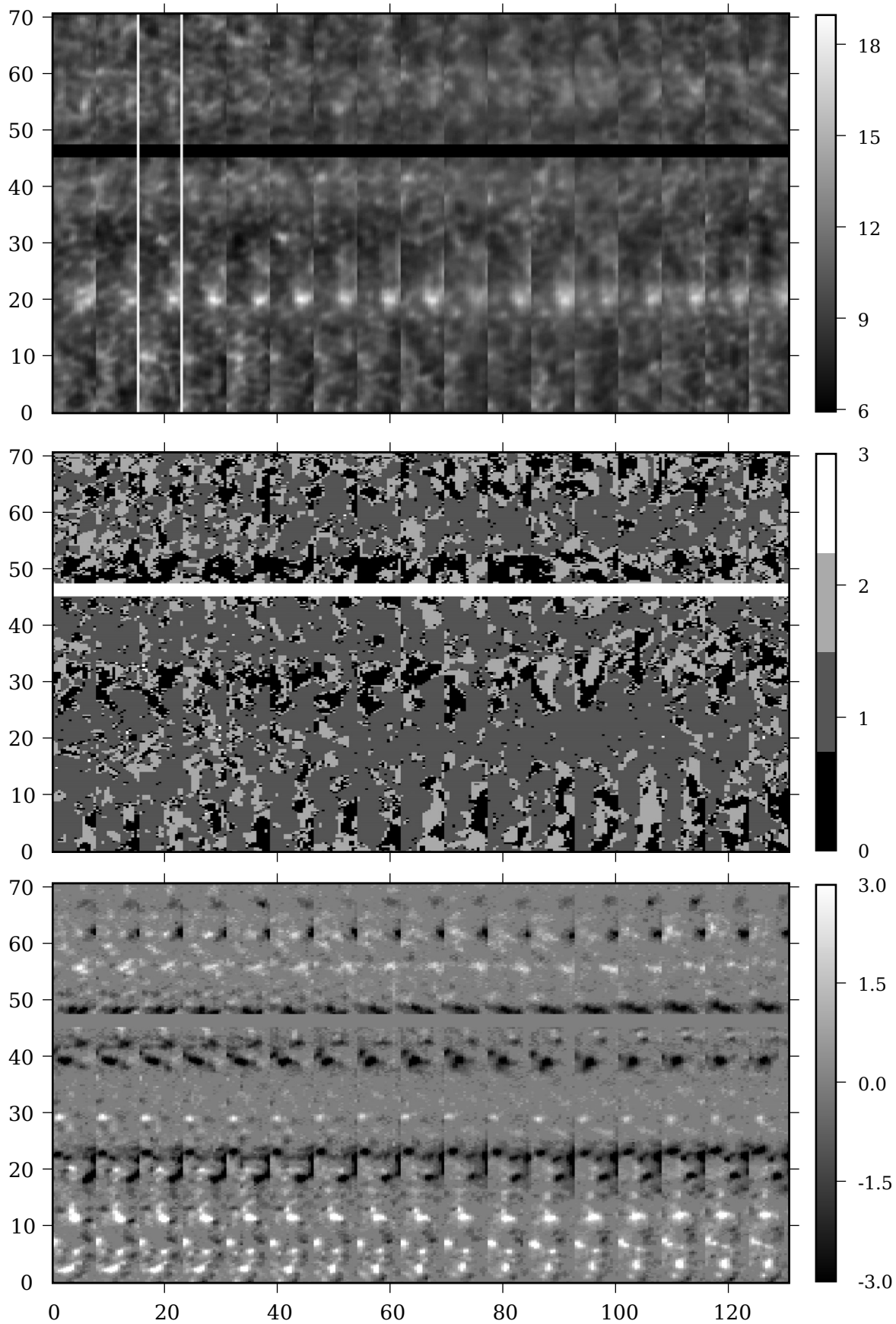
Fig. 1. Maps of the observed area. *Top*: H-index in pm; *middle*: profile type. It is coded as follows: 0: reversal-free; 1: normal; 2: asymmetric; 3: other types. *Bottom*: V_{tot}, which is a measure of the net vertical magnetic flux density (Lites et al. 1999) in arbitrary units. The x-axis shows both scanning direction and time (width of a single map is eight arcsec). The y-axis is the slit direction. Both axes are in arcsec. Only 17 out of 40 scans are shown here. The time duration per scan was about 100 s.
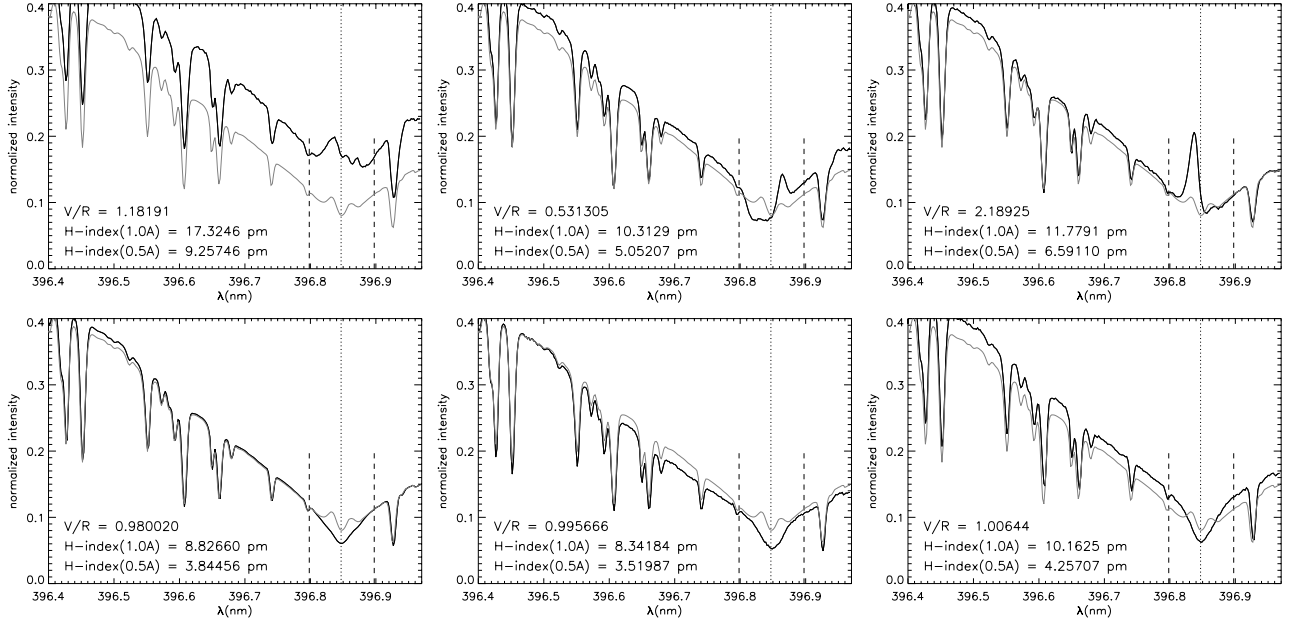
Fig. 2. Examples of single calcium profiles with drastically different properties observed in the quiet Sun. The gray profile is the average of a few thousand profiles (cell interior and boundary). *Top left*: a profile with three emission peaks. *Top middle*: a very asymmetric profile with only a red emission peak. *Top right*: a very asymmetric profile with two emission peaks. *Bottom*: three reversal-free profiles. Note the level of the wing intensity with respect to the wing of the average profile. The dashed lines show a distance of ±0.05 nm from the average calcium core, indicated by a vertical dotted line. *The bottom left profile* is an average of 59 reversal-free profiles while the other panels show single profiles. Except for *the top middle and right panels*, the *V/R* ratio was calculated using bands.
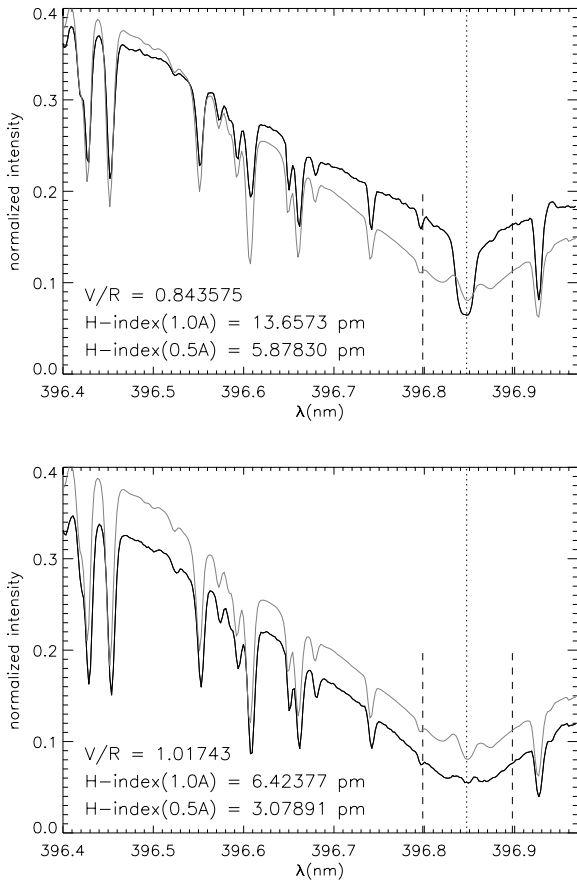

Fig. 3. These two examples show that the integrated intensity close to the core, either H-index or a filter, is not a reliable criterion to separate reversal-free profiles from profiles with emission peaks. Positions (in Fig. 1) of *the upper and lower profile* are (18.7, 30.5) and (32.6, 30.2), respectively.

lateral radiative transfer to play a role. In addition, we use the microturbulence values as specified with the semi-empirical models we employ, even though we do not know anything about the unresolved small-scale velocities in the observed features. Synthetic profiles from semi-empirical 1D quiet-Sun models with non-zero microturbulence tend to have H_2-peaks that are generally stronger than observed; using zero microturbulence, as one would do if the structure to be modeled were completely resolved, would only widen this discrepancy. Since we cannot be sure that the structure is completely resolved in the observations, and also because we expect that radiative interaction with the environment will lead to broadening of the H_2-peaks, we decided not to change the microturbulent velocities. Note that the latter is not an observational effect, but solely due to scattering of line photons in the solar atmosphere.

As model atmospheres we use four semi-empirical models: FALC (quiet Sun) and FALA (inter-network) from Fontenla et al. (1999, 2006); the Holweger-Müller atmosphere (Holweger & Müller 1974), which is very similar to a theoretical radiative equilibrium model, but not constructed to strictly satisfy this condition; and the new C6 quiet Sun model atmosphere, provided in advance of publication (Avrett & Loeser 2008, where this model is now called C7). The left panel of Fig. 4 shows the temperature stratification of these four model atmospheres. All of the models, except the Holweger-Müller model, show a chromospheric temperature rise at different heights in the atmosphere. The Holweger-Müller model has a monotonically-decreasing temperature stratification with an artificial extension with constant slope (almost isothermal). The extension is required to include the formation height of the Ca II resonance lines. The synthesized calcium profiles are shown in the right panel of Fig. 4. For comparison, the reversal-free profile from the bottom left panel of Fig. 2 is overplotted in gray.

For all synthesized profiles, except the one derived from the Holweger-Müller model, there are well-defined emission peaks
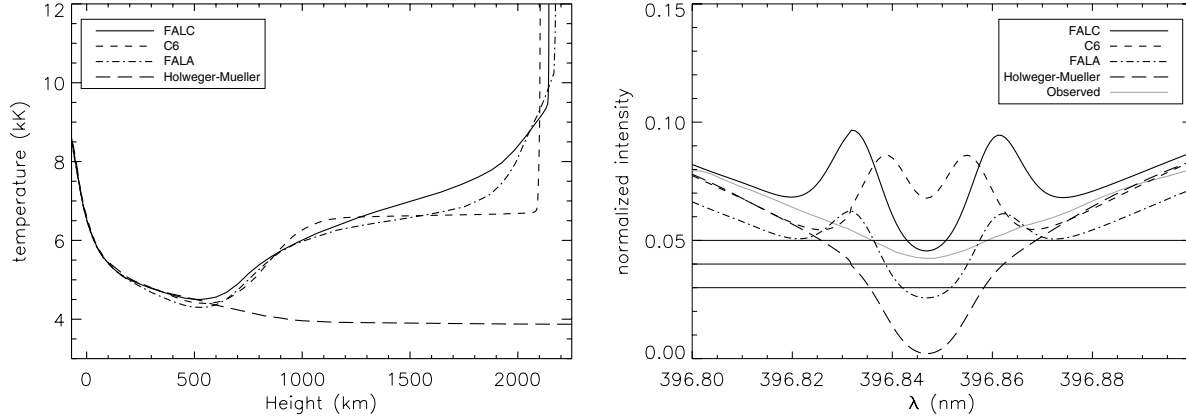
Fig. 4. *Left*: stratification of the temperature in the FALA, FALC, Holweger-Müller, and C6 model atmospheres. *Right*: resulting calcium profiles. Except for the Holweger-Müller model atmosphere, which does not show a temperature rise, all model atmospheres result in two emission peaks. We set the nearby pseudo-continuum of the FALC profile to unity and use this normalization factor for all synthetic profiles. The observed reversal-free profile in *the bottom left panel* of Fig. 2 is shown in gray. All synthetic profiles convolved to the spectral resolution of the observed spectra; scattered light removed from the observed profiles.

at the H_{2v} and H_{2r} wavelengths. All the synthetic profiles are significantly different from the observed reversal-free profiles. It might suggest that, e.g., the temperature rise in the chromosphere is either shifted to higher layers, or the temperature gradient is not as steep as proposed by, for example, the C6 model. For a very inhomogeneous model atmosphere, the region with high emission may be very "patchy".

The new chromospheric model C6, like FALC, includes a chromospheric temperature rise. If one considers a velocity stratification in the atmosphere, it will be possible to reproduce a variety of asymmetric calcium profiles (e.g., Heasley 1975). However, it is not trivial to diminish both emission peaks at the same time to reproduce a reversal-free profile. As seen in Fig. 4, none of the applied models with a chromospheric temperature rise produces a reversal-free calcium profile. While the C6, FALA, and FALC models look too hot, with strong emission peaks, the Holweger-Müller model fails due to its very deep calcium core. The dynamical models of Carlsson & Stein (1994, 1997) and Rammacher & Cuntz (2005) have episodes (significantly) cooler than the Holweger-Müller model with correspondingly lower line core intensities (Uitenbroek 2002; Rammacher 2005). It should be remembered, however, that the chromospheric radiative transfer in those simulations is not "consistent": important cooling agents are not represented at all and deviations from various equilibrium states are ignored.

4. Modified model atmospheres

Given the large deviations between all synthetic profiles of the Ca II H line and the observed reversal-free profiles, it is tempting to try to obtain a closer match to the observed profiles by making changes to one of the model atmospheres, specifically to the FALC model. This procedure is by no means unique and given that we employ static models it is not clear whether we can reproduce the observed profiles that result from the dynamic and highly-structured solar atmosphere. We could end up adjusting all atmospheric parameters and still not get a satisfactory match. Instead, we choose to adjust only the FALC temperature in a very schematic way to get at least an indication which changes might be needed. We stress, however, that these modified models are no longer consistent since only the temperature is changed and all other parameters are left intact. They may not reproduce
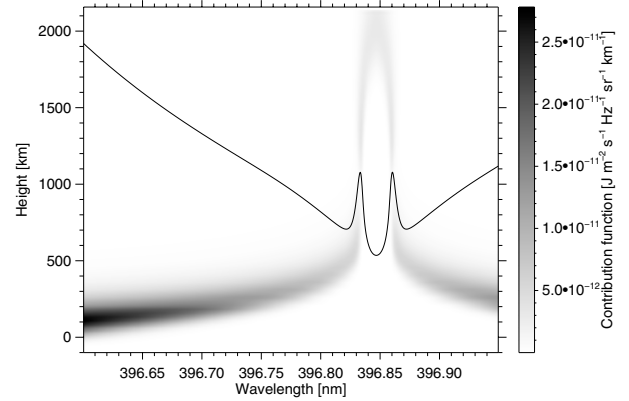

Fig. 5. Intensity contribution function for the inner part of the Ca II H line computed for the FALC model. The black line is the calcium profile of the model.

observed profiles of other lines. From the NLTE radiative transfer computations we know that the monochromatic source function follows the local temperature fairly well throughout most of the Ca II H line, even though it is a strong, scattering line. This means that a naive change of the temperature stratification at some height translates into a change in emergent intensity for those parts of the line that form at that particular height. The intensity contribution function for the Ca II H line (Fig. 5) indicates that the formation range for any given wavelength is very limited, which means that temperature corrections at a given height will lead to predictable line profile changes. This procedure should work particularly well for the line wings up to the H_1 minima, where the source function is very close to LTE, and for the very core, whose source function drops way below the Planck function in a predictable way. However, even though the formation range at any wavelength within the H_2 peaks is narrow, the wide range of formation heights spanned by these peaks as a whole necessitates temperature changes over a wide height range to suppress the emission peaks completely. In addition, we need a rather high temperature in the upper chromosphere to obtain a reasonable core intensity; for that reason we use the FALC model as starting point. This means that we may only change the temperature structure in the lower and middle chromosphere: we created models with the temperature
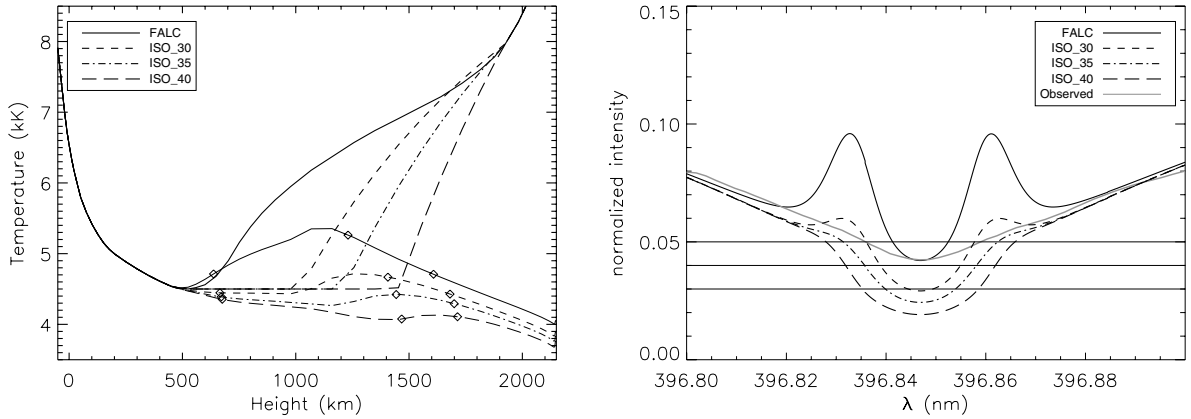
Fig. 6. *Left*: stratification of the temperature in the FALC model atmosphere and three modified versions of that. The thin curves represent the monochromatic source functions of these models at $\Delta\lambda = -0.014$ nm from line center. The diamonds (*from left to right* on each curve) represent the location of $\tau_\nu = 1$ for $\Delta\lambda = -0.016$, $\Delta\lambda = -0.014$, and $\Delta\lambda = -0.012$ nm. The source function is similar for all three wavelengths, so that we restrict to just one source function curve per model. *Right*: resulting calcium profiles of the mentioned models convolved to the spectral resolution of POLIS. The ISO_30 profile is much closer to the observed reversal-free profile than the FALC model.

minimum region isothermally extended upward to column mass values of $10^{-3.0}$ (ISO_30), $10^{-3.5}$ (ISO_35), and $10^{-4.0}$ (ISO_40), followed by a linear $T(\log m)$ relation up to a column mass of $m = 2 \times 10^{-5}$ g/cm^2, above which the original FALC temperatures are retained (Fig. 6, left panel). The lower temperature in the height range about 600−1900 km weakens the emission peaks, while the temperature rise in the higher layers prevents a very deep calcium core. The profiles (Fig. 6, right panel) suggest that a temperature rise shifted to larger heights is a step toward producing a reversal-free profile.

5. Discussion

We find that a quarter of all observed profiles are reversal-free profiles. We observed reversal-free profiles of the Ca II H line with an exposure time of about 4.8 s. However, they may get lost at longer exposure times. The maximum spatial extension of these reversal-free profiles in our map is about 5 arcsec; they mostly appear in smaller structures (Fig. 1, middle panel). The coherency of the position of the reversal-free profiles shows that they are not an artifact due to effects caused in the Earth atmosphere. The observed reversal-free Ca II H profiles (Fig. 2, lower panels) suggest that there may be some cool patches in the chromosphere for short periods of time. In contrast, Carlsson et al. (1997) tried to find reversal-free profiles in chromospheric spectral lines observed with SUMER (46.5−161 nm). On the basis of a few lines they concluded that "all chromospheric lines show emission above the continuum everywhere, all the time". These lines cover a large height range above the classical temperature minimum and should also reveal the cool patches seen in Ca II H line profiles if observed at the proper spatial and temporal resolution.

We propose that at a spatial resolution of one arcsecond, the average temperature stratification in the solar atmosphere is probably hotter than the Holweger-Müller model atmosphere, but still does not show a permanent temperature rise at all spatial positions. Moreover, the residual core intensity of these profiles is about 0.05 I_c. The Holweger-Müller model, as well as comparable cool models (like model Q of Solanki et al. 1991; or model COOLC of Ayres et al. 1986) and the cool phases of the dynamic models result in a very dark calcium core (Uitenbroek 2002), far below the observed reversal-free profiles. In these models, we have a longer cool phase and a shorter hot phase in

the chromosphere (Rutten 1998; Judge & Peter 1998). Statistics of our inter-network sample indicates that some 75% of all profiles show one or more clear emission peaks. This appears to be in conflict with these models. But we recall that even if at any given point in the atmosphere the temperature is low most of the time, the Ca II H line may still show emission peaks most of the time because it is an integral property with contributions from a large height range. We speculate that this is even more important in 3D models, where lateral interaction with the ubiquitous shocks plays a role as well. Unfortunately, so far no one has attempted to compute Ca II H profiles simultaneously with the 3D (M)HD simulations. Even worse, computing Ca II H a posteriori for a single 3D snapshot already presents an unsolved task.

On the other hand, our statistical studies of the inter-network calcium profiles indicate that about 25% of the profiles do not show any emission peak (but might show a bulge). These reversal-free profiles (bottom panels, Fig. 2) are not reproduced by any of the hydrostatic model atmospheres with a chromospheric temperature rise, like in the new C6 model. This challenges Avrett & Loeser (2008), who claim that they can reproduce all continuum and line intensities with models that have a temperature variation of at most 400 K. In addition, the observed reversal-free profiles cannot be derived from the dynamical models during the cool phase (Uitenbroek 2002, Fig. 6). Similarly, Avrett (1985) tried to modify the temperature stratification of VALA, VALC and VALF models to reproduce minimum and maximum profiles of Cram & Damé (1983). While we kept the temperature minimum constant and extended it isothermally, they introduced a hotter temperature minimum and decreased the temperature gradient (their Fig. 17). Our model ISO_30 and the corresponding profile (Fig. 6) better fits the observed reversal-free profile, which has lower intensity at the emission peak wavelengths than the minimum profile of Cram & Damé (1983).

Fontenla et al. (2007) presented a compromise solution for the cool patches. They proposed that cool patches may occur in a limited height range, such that they contribute substantially to the temperature sensitive molecules, but affect other spectral lines very little. This argument may apply to high resolution filtergrams (Wöger et al. 2006). If we had cool temperatures in a very limited height range as proposed by Fontenla et al. (2007), and a hot atmosphere elsewhere, we would see emission features somewhere in each Ca II H spectrum, which is not the case.

Therefore, although we have strong indications of cool patches in the solar chromosphere, they are more extended (in height) than was proposed by Fontenla et al. (2007).

Balasubramaniam (2001) presented multiple reversal calcium profiles and interpreted them as a signature of magnetic flux emergence. We observe some calcium profiles with more than two emission peaks (Fig. 2, upper left panel) in the quiet Sun, without signature of magnetic flux emergence in the polarimetric channel of POLIS (see Beck et al. 2008, for a description of this channel). Therefore, his explanation is not unique.

6. Conclusion

We find that a quarter of the observed calcium profiles in the quiet Sun inter-network show a reversal-free pattern. We interpret these profiles as strong indication for a temperature stratification cooler than that of the average quiet Sun. Although they do not imply a very cool atmosphere, like the one based on CO line observations (Ayres 2002) and numerical simulations (e.g., Carlsson et al. 1997; Rammacher & Cuntz 2005), it should be clearly cooler than was suggested by Avrett & Loeser (2008). The reversal-free profiles we observe, at a spatial resolution of 1 arcsec and a temporal resolution of 5 s, show a residual intensity at the core of about 0.05 I_c. Hence, the profiles suggest that the cool components are cooler than the FALA, FALC, and C6 models in the sense that their corresponding profiles do not have any emission peak, but hotter than the extended Holweger-Müller model or the cool phase in the dynamic models.

References

Avrett, E. H. 1985, in Chromospheric Diagnostics and Modelling, NSO/SP Summer Conf., Sunspot, ed. B. W. Lites, 67
Avrett, E. H. 2007, in The Physics of Chromospheric Plasmas, ed. P. Heinzel, I. Dorotovič, & R. J. Rutten, ASP Conf. Ser., 368, 81
Avrett, E. H., & Loeser, R. 2008, ApJS, 175, 229
Ayres, T. R. 2002, ApJ, 575, 1104
Ayres, T. R., Testerman, L., & Brault, J. W. 1986, ApJ, 304, 542
Balasubramaniam, K. S. 2001, ApJ, 557, 366
Beck, C., Schmidt, W., Kentischer, T., & Elmore, D. 2005, A&A, 437, 1159
Beck, C., Schmidt, W., Rezaei, R., & Rammacher, W. 2008, A&A, 479, 213
Carlsson, M., & Stein, R. F. 1994, in Chromospheric Dynamics, ed. M. Carlsson, 47
Carlsson, M., & Stein, R. F. 1997, ApJ, 481, 500
Carlsson, M., Judge, P. G., & Wilhelm, K. 1997, ApJ, 486, L63
Cram, L. E., & Damé, L. 1983, ApJ, 272, 355
Fontenla, J., White, O. R., Fox, P. A., Avrett, E. H., & Kurucz, R. L. 1999, ApJ, 518, 480
Fontenla, J. M., Avrett, E., Thuillier, G., & Harder, J. 2006, ApJ, 639, 441
Fontenla, J. M., Balasubramaniam, K. S., & Harder, J. 2007, in The Physics of Chromospheric Plasma, ed. P. Heinzel, I. Dorotovič, & R. J. Rutten, ASP Conf. Ser., 368, 499
Grossman-Doerth, U., Kneer, F., & von Uexküll, M. 1974, Sol. Phys., 37, 85
Heasley, J. N. 1975, Sol. Phys., 44, 275
Holweger, H., & Müller, E. A. 1974, Sol. Phys., 39, 19
Judge, P. G., & Peter, H. 1998, Space Sci. Rev., 85, 187
Kalkofen, W., Ulmschneider, P., & Avrett, E. H. 1999, ApJ, 521, L141
Linsky, J. L., & Avrett, E. H. 1970, PASP, 82, 169
Lites, B. W., Rutten, R. J., & Kalkofen, W. 1993, ApJ, 414, 345
Lites, B. W., Rutten, R. J., & Berger, T. E. 1999, ApJ, 517, 1013
Rammacher, W. 2005, in Chromospheric and Coronal Magnetic Fields, ed. D. E. Innes, A. Lagg, & S. K. Solanki, ESA Special Publication, 596, 60
Rammacher, W., & Cuntz, M. 2005, A&A, 438, 721
Rezaei, R., Schlichenmaier, R., Beck, C. A. R., Bruls, J. H. M. J., & Schmidt, W. 2007a, A&A, 466, 1131
Rezaei, R., Schlichenmaier, R., Schmidt, W., & Steiner, O. 2007b, A&A, 469, L9
Rutten, R. J. 1998, in Solar Composition and Its Evolution – From Core to Corona, ed. C. Fröhlich, M. C. E. Huber, S. K. Solanki, & R. von Steiger, 269
Schmidt, W., Beck, C., Kentischer, T., Elmore, D., & Lites, B. 2003, Astron. Nachr., 324, 300
Shine, R. A., & Linsky, J. L. 1974, Sol. Phys., 39, 49
Solanki, S. K., Steiner, O., & Uitenbroek, H. 1991, A&A, 250, 220
Stenflo, J. O., Solanki, S., Harvey, J. W., & Brault, J. W. 1984, A&A, 131, 333
Uitenbroek, H. 1989, A&A, 213, 360
Uitenbroek, H. 2001, ApJ, 557, 389
Uitenbroek, H. 2002, ApJ, 565, 1312
Vernazza, J. E., Avrett, E. H., & Loeser, R. 1981, ApJS, 45, 635
von der Lühe, O., Soltau, D., Berkefeld, T., & Schelenz, T. 2003, in Innovative Telescopes and Instrumentation for Solar Astrophysics, ed. S. L. Keil, & S. V. Avakyan, Proc. SPIE, 4853, 187
Wedemeyer-Böhm, S., Freytag, B., Steffen, M., Ludwig, H.-G., & Holweger, H. 2004, A&A, 414, 1121
Wedemeyer-Böhm, S., Kamp, I., Bruls, J., & Freytag, B. 2005, A&A, 438, 1043
Wöger, F., Wedemeyer-Böhm, S., Schmidt, W., & von der Lühe, O. 2006, A&A, 459, L9